

Cite this: *Mater. Adv.*, 2025,  
6, 1842

# Flexible polyurethane foam: materials, synthesis, recycling, and applications in energy harvesting – a review

Ahmed Abdelhamid Maamoun,<sup>a</sup> Mustafa Arafa<sup>id</sup><sup>b</sup> and Amal M. K. Esawi<sup>id</sup>\*<sup>b</sup>

The increasing demand for sustainable and clean energy, driven by the finite supply of fossil fuels, has motivated researchers to explore alternative energy sources. Triboelectric nanogenerators (TENGs) are innovative devices that convert mechanical energy into electrical energy without the use of an external power source. The efficiency of TENG devices relies heavily on the materials employed. Polymeric materials with porous structures have proved particularly effective for TENG applications. Among these, polyurethanes (PUs) stand out as a versatile class of materials with significant potential across various applications, owing to their unique structure–property relationships. Flexible polyurethanes (FPUs) exhibit high elasticity, a three-dimensional pore network, and diverse densities that make them a promising material for energy harvesting applications. This review explores the materials, chemistry, recycling, and limitations of FPUs with a focus on their application in TENG devices. Furthermore, it compares the efficiency of FPUs in TENG devices with compact and other porous materials. The review concludes that FPU is a promising material for TENG devices across a wide range of applications, outperforming compact materials. This is mainly due to several advantages, such as high porosity, high elasticity, lightweight nature, versatility, durability, and cost-effectiveness. In addition, this review presents the future scope for the use of FPU in TENG applications.

Received 13th October 2024,  
Accepted 12th February 2025

DOI: 10.1039/d4ma01026d

rsc.li/materials-advances

## 1. Introduction

Polyurethane (PU) foams have gained recognition in a wide range of industries since their discovery by Otto Bayer and his co-workers in 1947.<sup>1</sup> PU is a synthetic polymer formed through the reaction of polyol (R-(OH)<sub>n≥2</sub>) and isocyanate (R-(NCO)<sub>n≥2</sub>).<sup>2,3</sup> These versatile materials find applications in coatings,<sup>4,5</sup> adhesives,<sup>6,7</sup> sealants,<sup>8,9</sup> elastomers,<sup>10,11</sup> construction,<sup>12</sup> packaging,<sup>13,14</sup> automobiles<sup>15</sup> and energy harvesting.<sup>16</sup> Nowadays, PUs have become ubiquitous in everyday products and are regarded as essential classes of polymers that enhance human well-being.<sup>17</sup> According to statistics, it is estimated that by 2030, the global PU market will be worth approximately 112.45 billion USD.<sup>18</sup>

The properties displayed by PUs are typically affected by the specific types of polyols and isocyanates used in their production.<sup>19</sup> For instance, polyether polyols contribute flexibility, while polyester polyols enhance hardness and strength. Similarly, the choice of isocyanates, whether aliphatic or

aromatic, influences the final properties of the PUs. This diversity in formulation allows for a wide range of applications, making the market for PU products virtually limitless.<sup>20,21</sup> Flexible polyurethane (FPU) foam is characterized by its open cell morphology, high elasticity, light weight and versatility, and thus it can be employed in different applications such as bedding,<sup>22,23</sup> automobiles,<sup>24–26</sup> sound absorption,<sup>27–29</sup> furniture,<sup>22</sup> and energy harvesting.<sup>30</sup> FPU is manufactured by introducing blowing agents, catalysts and stabilizers during the reaction between polyol and isocyanate, resulting in a cellular structure with a three-dimensional interconnected pore network.<sup>3</sup> Table 1 summarizes the role of each component in PU formulations. By adjusting the formulation and processing parameters, manufacturers customize the foam's physical and mechanical properties, such as density, and compression resistance to align to specific applications.

In recent years, many researchers have focused on utilizing FPU foams for energy harvesting applications to produce sustainable energy. Energy harvesting is a cutting-edge technology that captures energy from environmental sources, including those produced by natural or human activities, and transforms it into usable alternating current, thereby providing a sustainable power supply for portable systems.<sup>38</sup> This approach effectively leverages various energy sources, including fluid,<sup>39</sup> solar,<sup>40</sup>

<sup>a</sup> Department of Engineering Physics and Mathematics, Chemistry Division, Faculty of Engineering, Ain Shams University, 1 EL-Sarayat Street – Abdo Basha Sq., Cairo, 11517, Egypt

<sup>b</sup> Department of Mechanical Engineering, The American University in Cairo, AUC Avenue, P.O. Box 74, New Cairo 11835, Egypt. E-mail: a\_esawi@aucegypt.edu



Table 1 The role of each component in PU formulation

Material	Role	Ref.
Polyol	Provides soft, flexible segments in PUs	31
Isocyanate	Enables the curing or hardening process of PUs	32
Surfactant	Stabilizes the foam's cellular structure	33
Catalysts	Accelerate the chemical reactions at lower temperatures, speeding up production	34
Blowing agent	Generates the foam architecture and controls the foam's level	33
Filler	Enhances mechanical properties like strength and durability, while reducing material costs	35
Flame retardancy	Reduces the flammability of the material, improving safety	36
Pigments	Add color to the material, enhancing its aesthetic appeal	37

wind,<sup>41</sup> thermal,<sup>42–44</sup> and mechanical energy.<sup>45</sup> Among these, mechanical energy stands out due to its abundance and reliability, as it remains largely unaffected by fluctuations in weather conditions.<sup>46</sup> Among the various forms of mechanical energy, triboelectric nanogenerators have garnered considerable interest from researchers due to their remarkable efficiency and adaptability. Using triboelectric nanogenerators (TENGs) is a novel approach that enables the conversion of mechanical energy, such as vibrations or movements, into electrical energy without relying on external power sources.<sup>47–49</sup> The efficiency and performance of TENG devices are influenced by various factors, including the materials used, contact area, frequency, and applied force. The utilization of FPU foam as a triboelectric layer in TENGs represents a significant advancement in energy harvesting.<sup>16,48,50</sup> FPU foam exhibits remarkable characteristics that offer compelling substitutes for conventional metals, which often face limitations such as susceptibility to corrosion and unsuitability for prolonged use in TENG applications.<sup>51</sup> The foam's light weight, high elasticity, deformable nature and three dimensional pore structure enable more significant surface contact and friction between triboelectric layers, improving energy harvesting efficiency.<sup>52</sup> These advantages make FPU foam suitable for applications such as wearable electronics, self-powered sensors, and portable devices, contributing to advancements in sustainable energy harvesting.

In this review, the application of FPU in TENGs is highlighted. Insights are provided into the materials and chemistry of FPU foams, aiming to deepen the understanding of the structure–property relationship. Furthermore, it covers recycling methods for polyurethane waste. This review also explores how FPU foams can effectively generate electricity through triboelectric effects. Additionally, it discusses the limitations and prospects of utilizing FPU in this application.

## 2. Materials

### 2.1. Polyols

Polyols are a versatile and innovative class of polymeric materials that have revolutionized the foam industry.<sup>31</sup> They are widely used in the production of PU materials. They provide the fundamental framework for manufacturing high-quality, durable, and comfortable foam products that are integral to our daily lives.<sup>53</sup> Typically, these compounds are derived from either crude oil or natural oil from renewable sources and contain two or more hydroxyl (–OH) groups, which provide

the necessary reactive sites for forming PU foam.<sup>54</sup> There are two primary categories of polyols: polyether and polyester polyols.<sup>55</sup> Fig. 1 illustrates the base-catalyzed ring opening polymerization reaction for ethylene oxide (EO) and propylene oxide (PO) that produces polyether polyol. On the other hand, polyester polyol is produced through the reaction of diacids and diols (as depicted in Fig. 2).<sup>56</sup> There are numerous varieties of polyols, each with distinctive advantages and properties that make them suitable for various applications.

The ability of polyols to impart flexibility and resilience to the final product is a major factor that makes them desirable to produce FPU foam. By carefully selecting the type and composition of polyols, manufacturers can tailor the foam's properties to satisfy specific needs,<sup>57</sup> such as varying the densities, compression factors, and load-bearing abilities.

**2.1.1. Polyether polyols.** EO and PO are indispensable monomers in the synthesis of polyether-based polyols, which are extensively employed in the FPU industry. The polymerization of both oxides can be carried out *via* the base-catalyzed ring opening technique. This method employs an initiator with active hydrogen atoms such as water, glycerin, ethylene glycol, sorbitol, or ethylene diamine and a catalyst like potassium hydroxide. Fig. 1 depicts base-catalyzed ring opening polymerization for EO and PO. The resulting polyether polyol has linear or branched chains with ether (–O–) moieties. Furthermore, the resulting polymer from EO exhibits primary hydroxyl groups, while the polymer derived from PO possesses secondary hydroxyl groups due to the greater accessibility of the less hindered carbon in the ring to nucleophilic attack.<sup>31,58–60</sup>

**2.1.2. Polyester polyols.** Polyester polyols are essential components in the PU industry, considered essential building



R: Alkyl group



Fig. 1 The base-catalyzed ring opening polymerization for EO and PO.





Fig. 2 Schematic representation for polyester polyol preparation.

blocks in the synthesis of PU for use in coatings, adhesives, sealants and elastomer applications.<sup>61</sup> Polyester polyols are produced by the polycondensation between diols and dicarboxylic acids or their derivatives.<sup>21</sup> Fig. 2 reveals the typical schematic protocol for polyester polyol preparation. Although this reaction can occur without catalysts, optimal results in terms of reduced acidity levels and accelerated reaction times are obtained when specific catalysts are employed.<sup>62</sup> Notable catalysts include tin compounds (stannous octoate),<sup>63</sup> *p*-toluene sulfonic acid,<sup>64</sup> and zinc acetate.<sup>65</sup> The polyester-based PU foams are favored in the construction and insulation industries due to their superior insulating properties, mechanical performance, dimension stability, and durability.<sup>20</sup> Additionally, polyester polyols are used extensively to formulate PU coatings and adhesives.<sup>66</sup> The presence of ester (–COO) groups in the polyester structure gives the resultant coatings and adhesives excellent adhesion properties. Furthermore, polyester-based PU coatings offer excellent resistance to abrasion, chemicals, harsh environments, and a lustrous and smooth surface, making them suitable for various bonding applications.<sup>67,68</sup>

Polyester polyols' versatility extends to the PU elastomer industry as well. Polyester polyol-based elastomers exhibit remarkable mechanical properties, including high tensile strength and tear resistance. These elastomers are utilized in numerous industries, including automotive, footwear, and industrial manufacturing, where the combination of durability and flexibility is crucial.<sup>69</sup> Therefore, the choice between polyether and polyester polyols for manufacturing PU foam depends on the specific needs of the application, such as the desired foam properties and environmental conditions. Table 2 provides a comparison between polyether and polyester polyols.

**2.1.3. Bio-based polyols.** Biobased polyols are renewable and sustainable materials that have received considerable attention in polymer science.<sup>71</sup> These polyols are derived from biomass feedstocks, including plant oils, agricultural residue, and other renewable resources, making them a viable alternative to petroleum-based polyols. In 2022, the bio-based FPU foam industry achieved a noteworthy market share of 50.0% when compared to other PU products.<sup>72</sup> This achievement can

be attributed to its extensive applications as a cushioning material in various consumer and commercial goods, such as carpet underlay, beds, furniture, automotive interiors, and packaging.<sup>73</sup>

Several processes, including transesterification,<sup>74</sup> epoxidation,<sup>75</sup> and ring-opening polymerization<sup>76</sup> are required for the production of biobased polyols. These processes transform the biomass feedstock into polyol structures with desirable properties. Numerous advantages are associated with bio-based polyols, including reduced environmental impact, decreased reliance on fossil fuels, and the potential for enhanced biodegradability.<sup>77</sup> In addition, their incorporation into PU formulations enhanced the mechanical properties, thermal stability, and overall performance of the material.

Numerous studies have explored the use of vegetable oil-based polyols, including castor oil,<sup>78,79</sup> soybean oil,<sup>80,81</sup> palm oil,<sup>82,83</sup> rapeseed oil,<sup>84,85</sup> tung oil,<sup>86,87</sup> and sunflower oil<sup>88</sup> in the production of PUs. Among them, castor and soybean oils are the most common feedstocks used in the PU industry to produce biobased polyols. Castor oil, extracted from the seeds of the castor plant, has become an essential raw material for biobased polyol synthesis. Castor oil, which is abundant in hydroxyl functional groups, is made suitable for direct use as a polyol precursor in the synthesis of PUs without the need for any thermochemical modification. Its distinctive chemical structure, which consists of a hydrophobic fatty acid chain and hydroxyl group functionality, imparts desirable properties to the resulting PU materials, such as increased crosslinking, enhanced mechanical performance, and superior water resistance. On the other hand, soybean oil derived from soybeans is a readily available and inexpensive feedstock that can be rapidly converted into polyols *via* epoxidation then ring opening.<sup>89</sup>

The epoxidation of double bonds, which are present in the backbone structure of soybean oil, is crucial for transforming an unsaturated oil into a polyol. The mechanism of soybean epoxidation is illustrated in Fig. 3a. Typically, soybean oil is epoxidized by reacting the double bonds of the oil with a peroxy acid, such as peroxyacetic acid (CH<sub>3</sub>CO<sub>3</sub>H). This acid is generated *in situ* by reacting hydrogen peroxide with acetic acid in the presence of a mineral acid catalyst.<sup>90</sup> The formation of

Table 2 General comparison between polyether and polyester polyols<sup>21,31,70</sup>

Characteristic	Polyether polyols	Polyester polyols
Chemical structure	Linear or branched chain with ether (–O–) linkages	Linear chain with ester (–COO) linkages
Reactivity	Low viscosity, higher reactivity	Higher viscosity, slower reactivity
Hydrolytic stability	Excellent hydrolytic stability	Lower hydrolytic stability
Characteristics	Flexible	Stiffness
Markets	Furniture, sound absorption	Insulation, coating, adhesives





Fig. 3 Schematic representation of (a) epoxide ring formation and (b) different protocols for epoxide ring opening.

polyols from epoxides can occur *via* four distinct mechanisms: acid reaction, hydrolysis, alcoholysis, and hydrogenolysis, as shown in Fig. 3b. In the mechanism of the acidic reaction, the epoxide ring is cleaved, resulting in the formation of polyols with chlorohydrin, bromohydrin, or hydroxyalkyl ester structures. The epoxide undergoes this transformation by reacting with HCl, HBr, or various organic acids ( $\text{R}-\text{COOH}$ ), respectively. On the other hand, the hydrolysis of epoxide rings with acidic catalysts such as sulfuric acid, *p*-toluene sulfonic acid, or phosphoric acid produces polyol with two vicinal hydroxyl groups. Additionally, the alcoholysis reaction utilizes excess alcohols and acidic catalysts to react with epoxidized rings, resulting in the formation of polyols. Finally, the hydrogenolysis of epoxidized oil to

produce polyols entails exposing the compound to pressurized gaseous hydrogen (approximately 4.1–6.9 MPa) in the presence of a catalyst such as RANEY<sup>®</sup> Ni.<sup>91</sup>

## 2.2. Isocyanates

Isocyanates ( $-\text{NCO}$ ), known for their versatility and high reactivity, play a central role in PU chemistry. Two of the most common diisocyanates used in the production of PU foam are toluene diisocyanate (TDI) and methylene diphenyl diisocyanate (MDI). TDI is a mixture of 2,4-TDI and 2,6-TDI, whereas MDI exists in various isomeric forms, including 2,2'-MDI, 2,4-MDI, and 4,4'-MDI. Isocyanates react with polyols in the presence of catalysts, surfactants, and a water-blowing agent to form a three-dimensional network structure with interconnected pores. This crosslinking reaction imparts FPU foam with its desired physical properties, such as elasticity, resilience, and durability.<sup>92</sup>

The production of TDI typically involves three steps. Fig. 4 illustrates the protocol for preparing TDI. Initially, toluene is nitrated to produce a mixture of 2,4- and 2,6-nitrotoluene isomers. The nitration procedure involves reacting toluene with concentrated nitric acid ( $\text{HNO}_3$ ) and sulfuric acid ( $\text{H}_2\text{SO}_4$ ), followed by separating and purifying the nitrotoluene isomers. The second step involves the catalytic hydrogenation of the nitrotoluene mixture, also known as the “reduction” process. Hydrogen gas and a metal catalyst, typically palladium, convert the nitrotoluene isomers into the corresponding toluene diamines. The toluene diamines are then reacted with phosgene ( $\text{COCl}_2$ ) to generate TDI, a mixture of 2,4- and 2,6-TDI isomers. In order to obtain the desired product, the resultant TDI mixture is purified to obtain specific isomer ratios.<sup>92,93</sup>

On the other hand, MDI is prepared through a two-step reaction of aniline and formaldehyde, followed by phosgenation, as demonstrated in Fig. 5. The first step is to condense aniline and formaldehyde to form methylene diphenyl diamines (MDAs). A suitable acid catalyst such as hydrochloric acid (HCl) is present during this stage under controlled temperature and pressure conditions. This reaction generates three principal isomers: 2,2'-MDA, 2,4'-MDA, and 4,4'-MDA. Depending



Fig. 4 Preparation scheme of TDI.





Fig. 5 Preparation scheme of MDI.

on the concentration of the acid catalyst, the process temperature, and the aniline-to-formaldehyde ratio, various amounts of these products are produced. In the second phase of the process, the mixture of MDA isomers is phosgenated with  $\text{COCl}_2$ , using chlorobenzene as a solvent, to form MDI. Phosgene and other chemical reactions are hazardous, so MDI synthesis is subject to strict safety and environmental regulations.<sup>94</sup> Table 3 compares the physical properties of TDI and MDI. MDI differs from TDI in terms of physical properties and isocyanate contents. Thus, it is essential to select the appropriate isocyanate based on the required degree of crosslinking, resilience, density, reactivity, and desired application.

### 2.3. Catalysts

The production of PU foam necessitates the use of catalysts to speed up the reaction between polyol and isocyanate, as well as to regulate the exothermic reaction and the polymerization

process.<sup>95</sup> The formulation of FPU foams involves two primary reactions: the gelling reaction and the blowing reaction. In the gelling (or polymerization) reaction, diisocyanates react with polyols to form urethane linkages. On the other hand, in the gas-producing (or blowing) reaction, the isocyanate reacts with water to form polyurea and carbon dioxide ( $\text{CO}_2$ ) gas. The kinetics of these reactions differ, dependent upon temperature, catalyst type, catalyst concentration, and various other factors. However, to produce high-quality foams, the rates of both reactions must be balanced and controlled.<sup>27,96–98</sup>

Suppose the blowing reaction occurs faster than the gelling reaction. In that case, the gas produced by the reaction may expand before the polymer is strong enough to contain it, and internal splits and foam collapse can occur. In contrast, if the polymerization occurs faster than the gas-producing reaction, the foam cells remain closed, causing the foam to shrink as it cools.<sup>99</sup> Uniform open cells will dominate the foam structure if these two reactions are balanced appropriately. Open cells offer

Table 3 Comparison between TDI and MDI<sup>92</sup>

Characteristics	TDI	MDI
Apparent color	Colorless to pale yellow	Brown
$M_{wt}$ ( $\text{g mol}^{-1}$ )	174.20	250.25
Structure	Mixture of 2,4- and 2,6-TDI	Mixture of 2,2', 2,4'- and 4,4'-MDI
Viscosity	Lower viscosity	Higher viscosity
Reactivity	More reactive	Less reactive
Toxicity	More toxic	Less toxic
Density	Moderate density	High density
Uses	Mainly to produce FPU foam	Mainly to produce semi-rigid and rigid PU foam



little resistance to diffusion, and the cell pressures quickly equilibrate without significant foam shrinkage.<sup>99</sup> Thus, there are two main types of catalysts typically used in the production of FPU foam to balance both reactions: metal-based catalysts and amine-based catalysts.

**2.3.1. Metal-based catalyst mechanism.** In FPU foam production, stannous octoate (tin(II) 2-ethylhexanoate) is often used as a gelling catalyst to accelerate the polymerization reaction. Stannous octoate acts as a Lewis acid and is generally believed to function by interacting with basic sites in both  $-NCO$  and  $-OH$  compounds. A lack of gelling catalyst will result in foam splitting or collapse if the polymer does not polymerize sufficiently. Conversely, using excessive gelling catalyst will result in closed cells and shrinkage.<sup>20,100</sup> Consequently, the crosslinking reaction catalyzed by stannous octoate plays a pivotal role in shaping the physical properties of the foam. This cross-linked structure enhances the foam's ability to retain its shape, withstand compressive forces, and resist tearing.

**2.3.2. Amine-based catalyst mechanism.** Among the widely utilized tertiary amine catalysts, one of the most prominent is 1,4-diazobicyclo[2,2,2]octane (DABCO), which effectively facilitates reactions involving isocyanate-polyol and isocyanate-water. However, tertiary amines have certain drawbacks, notably their unpleasant fishlike odor and high volatility. Considering the escalating environmental concerns surrounding reducing volatile organic compound (VOC) emissions, there has been a concerted effort to develop non-fugitive catalysts.<sup>97</sup> There are two suggested mechanisms for amine-catalyzed urethane formation. The first mechanism, proposed by Baker, suggests the creation of a complex comprising a tertiary amine catalyst and an isocyanate, followed by the nucleophile's attack (see Fig. 6a). The second is Farka's postulation, which involves the formation of urethane through catalyst protonation facilitated by the interaction of the amine with a proton source, polyol, to form a complex, which subsequently reacts with the isocyanate<sup>37</sup> (see Fig. 6b).

## 2.4. Blowing agents

Water is essential as a chemical blowing agent in all FPU foam formulations. However, its application requires meticulous consideration due to potential safety implications arising from excessive heat generation and associated fire hazards.<sup>95</sup> In the presence of isocyanate, water endures a chemical reaction that produces urea, biuret, and  $CO_2$  gas. This  $CO_2$  acts as a blowing agent, contributing to cell formation and expansion.<sup>31</sup> On the other hand, physical blowing agents with lower boiling points are utilized to create foam due to their ability to generate gas bubbles and assist in the formation of cellular structures within the polymer matrix. However, traditional physical blowing agents such as hydrocarbons and halocarbons pose significant environmental risks. Due to their chemical composition and physical properties, these substances have the potential to exacerbate global climate change by contributing to the destruction of the ozone layer and the intensification of the effects of greenhouse gases.<sup>101</sup>

## 2.5. Surfactant

A polydimethylsiloxane-polyether copolymer is widely employed as a surfactant in the manufacturing of FPU foams.<sup>102</sup> This silicon-based surfactant plays a crucial role in the production of FPU foam due to its multifaceted functions. Initially, it reduces surface tension, which aids in creating a more uniform and stable foam structure. Additionally, it emulsifies the polyol-isocyanate interface, enhancing compatibility between the ingredients and improving overall foam quality. Furthermore, it stabilizes cell windows, ensuring that the foam structure maintains its integrity and does not collapse during curing. Lastly, it promotes the generation of bubbles during mixing, resulting in a more homogeneous and controlled distribution of air bubbles within the foam.<sup>103</sup>

## 3. Basic chemistry of polyurethane

The urethane linkage ( $-NHCOO-$ ) is generated in PU chemistry by the reaction of an alcohol group ( $OH$ ) and an isocyanate

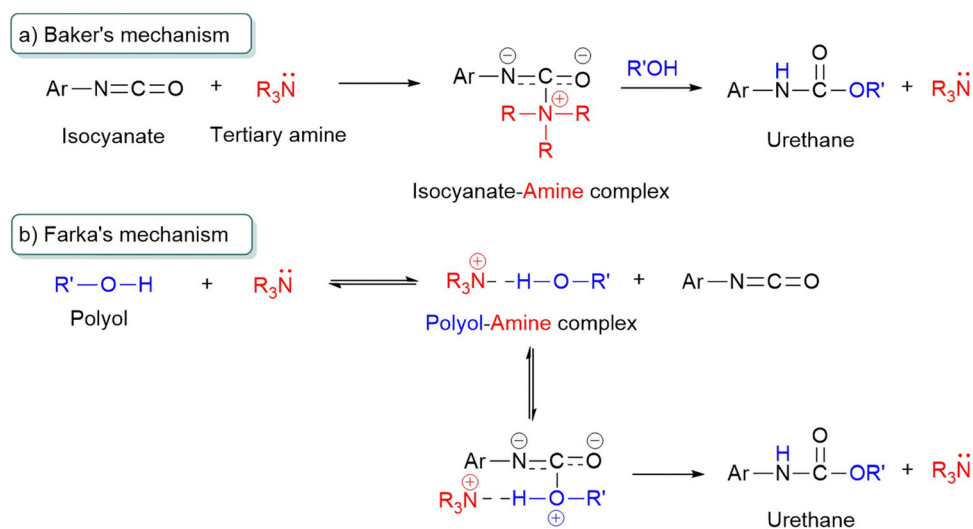


Fig. 6 Mechanisms of urethane formation catalyzed by tertiary amine: (a) Baker's mechanism, and (b) Farka's mechanism, adapted from ref. 97.



group (NCO). Understanding the isocyanate group is critical for understanding the entire process. Isocyanate molecules have the ( $-\text{N}=\text{C}=\text{O}$ ) group, and hydrogen atoms connected to atoms more electronegative than carbon are reactive to isocyanate. The isocyanate group's high reactivity with hydrogen-active compounds is explained by resonance configurations (Fig. 7a) in which the carbon atom has a low electron density, the oxygen atom has a high electron density, and the nitrogen atom has an intermediate negative charge. Isocyanates react with hydrogen-active substances through the carbon–nitrogen double bond ( $\text{N}=\text{C}$ ). The nucleophilic center of hydrogen-active compounds, such as the oxygen atom in hydroxyl groups or the nitrogen atoms in amines, attacks the electrophilic carbon atom. In contrast, hydrogen adds to the nitrogen atom in the  $-\text{NCO}$  groups. Additionally, electron-withdrawing groups increase  $-\text{NCO}$  group reactivity, whereas electron-donating groups decrease reactivity towards hydrogen-active substances. As a result, aromatic isocyanates ( $\text{R} = \text{aryl}$ ) are more reactive than aliphatic isocyanates ( $\text{R} = \text{alkyl}$ ). Furthermore, steric hindrance from adjacent groups can impair isocyanate reactivity.<sup>92,104</sup>

Several important reactions contribute to FPU foam formation, including urethane formation,  $\text{CO}_2$  and urea generation, and biuret formation. Urethane formation, named gelling reaction, is a fundamental reaction in PU foam synthesis (Fig. 7b). It is an

exothermic reaction that generates  $24 \text{ kcal mol}^{-1}$  of energy. It occurs when an NCO functional group reacts with a polyol's OH group. This reaction produces urethane linkages ( $-\text{NHCOO}-$ ), contributing to the foam's polymer backbone.<sup>31</sup>

The second most crucial reaction is the isocyanate–water reaction, known as the blowing reaction (Fig. 7c). This reaction is highly exothermic, releasing  $47 \text{ kcal mol}^{-1}$  of energy. During this reaction, isocyanate groups react with water to generate carbamic acid, which rapidly decomposes into  $\text{CO}_2$  and an amine. The resulting amine then reacts with NCO to produce urea moieties. Additionally, in the presence of urea, isocyanate can form a biuret linkage. Meanwhile, the  $\text{CO}_2$  gas produced during this reaction is responsible for the nucleation of bubbles within the PU matrix. These bubbles subsequently expand and stabilize throughout the curing process, forming the cellular structure of the PU foam.<sup>105,106</sup> The nucleation and growth of these bubbles determine the foam's final density, cell size, and mechanical properties.

## 4. Mechanism of cell formation and pore opening

Designing the pore structure of an FPU is crucial to meet the requirements of certain applications. The architecture of FPU



Fig. 7 Chemistry of FPU foam: (a) resonance configurations of isocyanate, (b) gelling reaction, and (c) blowing reaction.





Fig. 8 Schematic representation of the morphology of FPU foam, reproduced from ref. 107 with permission from Elsevier, copyright 2024.

foam consists of cavities (denoted by the orange circle) and pores, as shown in Fig. 8. The pores are categorized into three types: open, partially open, and closed pores.

Each type has unique properties that influence the foam's overall behavior. The inflation of the cavities occurs due to the rapid generation of CO<sub>2</sub> gases during the initial stages of the blowing process. These CO<sub>2</sub> molecules continue to inflate the cavities until they encounter other existing ones. As a result of the thin cavity walls' inability to withstand pressure from both sides, pores are formed. At this stage, the characteristics of the pores are significantly influenced by both the thickness of the cavity wall and the drainage flow rate. Due to the low wall strength compared to the cavity pressures and the high drainage flow rate, narrow cavity walls are predominantly characterized by the presence of open pores. On the other hand, if the cavity walls become denser, they tend to solidify at a reduced drainage flow rate before forming fully open pores, leading to a predominance of partially open pores. Additionally, the pores remain closed if the gelling reaction is completed before the cavity walls break.<sup>94,107</sup>

## 5. Modification of PU foams

Modifying FPU foam is crucial to meet specific needs and enhance its overall performance. There are two common techniques for PU modification. The first strategy involves applying a surface coating, a versatile method to enhance the properties and performance of FPU foam. Surface coatings serve as a protective layer on PU substrates, thereby boosting thermal stability, resistance to chemical attack, and environmental degradation. Various coating techniques, such as dip coating,<sup>108–110</sup> layer by layer self-assembly,<sup>111,112</sup> hydrothermal<sup>113,114</sup> or *in situ* polymerization<sup>115,116</sup> can accomplish uniform and controlled deposition of the coating material. Moreover, the selection of coating material can be customized to meet specific requirements, enabling functionalities like flame retardancy, antimicrobial properties, and UV protection. By carefully choosing the coating materials and fine-tuning the coating parameters, the mechanical, thermal, and surface properties of PU can be substantially improved, thus broadening the potential applications of PU-based materials across multiple industries.<sup>77,117</sup>

The second strategy focuses on adding fillers during FPU preparation. Fillers play a vital role in tailoring FPU properties by reinforcing the matrix and adding new functionalities.<sup>118</sup>

Strength, rigidity, and impact resistance can be enhanced by incorporating fillers into PU matrices. These fillers may be composed of either inorganic or organic substances, including nanoparticles and fibers. Inorganic fillers, such as montmorillonite,<sup>16</sup> silica,<sup>119</sup> alumina,<sup>120</sup> and carbon black,<sup>121</sup> are frequently used to improve mechanical properties, whereas organic fillers, such as cellulose<sup>122,123</sup> and wood,<sup>107,124</sup> offer benefits such as enhanced biodegradability and sustainability. It is important to optimize the filler type, particle size, and concentration to accomplish the desired cellular structure.<sup>125</sup> In addition, functional additives, such as flame retardants,<sup>126,127</sup> conductive materials,<sup>128</sup> and antimicrobial agents,<sup>3,129,130</sup> can be added to FPU matrices to impart specific properties for specialized applications. Overall, filler techniques provide an adaptable and effective method for customizing the properties of FPU-based materials to meet the requirements of various applications.

## 6. Mechanical performance of PU foams

The mechanical performance and durability of FPU foam are crucial considerations in various applications, especially in energy harvesting systems. The major drawback of PU foams is their relatively low mechanical strength, which restricts their usage.<sup>131</sup> The mechanical properties of FPU, including compression strength, tensile strength, tearing, resilience rate and elongation at break, can be modified by incorporating fillers during foam synthesis. Several studies have been conducted using natural organic and inorganic fillers with specific percentages to enhance the foam's mechanical properties. Utilizing natural fillers in PU foams presents a dual advantage: it enhances mechanical performance and mitigates the environmental challenges linked to natural solid waste materials. Furthermore, natural organic fillers possess a significant number of hydroxyl groups on their surface, which can strengthen physical interactions and hydrogen bonding with the PU matrix, thereby improving the mechanical performance of PU foams. Moreover, the high surface area and aspect ratio of nanofillers enable them to form strong interfacial bonds with the FPU matrix, which in turn promotes effective stress transfer when subjected to mechanical loads. This reinforcement restricts the mobility of PU chains, resulting in increased stiffness and strength. Furthermore, the uniform distribution of nanofillers throughout the PU matrix enhances stress distribution, leading to an increase in the mechanical performance of the foam.<sup>132</sup> However, the amount of filler must be carefully optimized, as an excessive quantity can lead to agglomeration, which compromises the flexibility and deformability of the FPU, adversely affecting the performance of the TENG during operation. Table 4 provides a summary of the impact of various natural fillers, including nanoparticles and fibers, on the mechanical properties of PU foams.

## 7. Recycling of PU waste

As environmental awareness grows, particularly in today's society which is focused on sustainable development, people



Table 4 Impact of different natural fillers on the mechanical properties of PUs

Filler	Optimal filler percentage (wt%)	Property enhanced	Enhancement (%)	Ref.
Palm oil fiber	5	Compressive strength	14.28	133
Nutmeg filler	1	Compressive strength	19	134
		Flexural strength	11	
		Impact strength	32	
Chitosan	5	Compressive strength	305.64	3
		Tensile strength	162.5	
Seashell	25	Compressive strength	71.42	118
Eggshell	20	Compressive strength	13	57
Chitin	2.5	Compressive strength	4.17	135
		Tensile strength	16.1	
Lignin	5	Tensile strength	18.6	135
Chitin-lignin	10	Compressive strength	5.56	135
		Tensile strength	14.4	
Rice plant waste	5	Tensile strength	7.2	136
Rice husk	1	Compressive strength	77.9	137
Silanized walnut shells	1	Compressive strength	15	131
		Tensile strength	9	
		Impact strength	6	
Artichoke stem waste fiber	5	Tensile strength	102	138
Sugar beet pulp	0.5	Compressive strength	6	139
Corncake waste	2	Tensile strength	23.46	140
Cellulose nanocrystals	4	Compressive strength	116	141
Na-MMT	0.3	Compressive strength	27.75	16
Sepiolite	5	Tensile strength	69.4	142
Organo modified MMT	3	Tensile strength	31.94	143
	5	Tear properties	284	
Organo modified bentonite	3	Tensile strength	17.94	143
	3	Tear properties	194	

are increasingly recognizing the strategic importance of resource conservation. Proper disposal and recycling of PU foam waste are essential for both environmental protection and cost reduction in production, as well as for improving material utilization. Due to its low density and high volume, PU foam waste is challenging to manage in landfills and incineration can produce hazardous gases. To address this issue, there are two primary methods for recycling PU foam waste (see Fig. 9): mechanical recycling and chemical recycling.<sup>144</sup>

### 7.1. Mechanical recycling

Mechanical recycling is a simple and cost-effective approach for reusing PU waste without requiring chemical treatment. This process involves several methods, including pressing with a binder, pressing without a binder, and regrinding. In the pressing with a binder method, which is the most common method used in industry, PU scrap is shredded to suitable sizes and mixed with a binder, typically isocyanate (MDI), in the presence of steam. The mixture is then compressed to achieve the desired density. The pressing without binder method involves bonding PU waste in the presence of heat and pressure. PU materials have soft segments that exhibit a thermoplastic nature within a temperature range of 150–220 °C. When heated to this temperature and under pressure, these segments can form mutual bonds. Finally, the regrinding process involves grinding PU waste into a powder form and reusing it as a filler in PU foam formulations.<sup>145</sup>

### 7.2. Chemical recycling

The urethane formation is a reversible reaction.<sup>31</sup> Chemical recycling involves the depolymerization of urethane into

monomers and low molecular weight oligomers in the presence of suitable reagents, heating, and catalysts. The polyol, isocyanate, and amines can be separated through a distillation process. The main techniques involved in the chemical recycling of PU waste, as shown in Fig. 9, are hydrolysis, acidolysis, aminolysis, and glycolysis.<sup>146</sup>

(i) **Hydrolysis.** This was the first method employed by Ford Motor Co. for the chemical recycling of PUs.<sup>147</sup> In this process, urethane linkages are depolymerized using an alkali metal hydroxide catalyst and steam. This results in the production



Fig. 9 Recycling methods for PU materials.



of polyols, amines, and CO<sub>2</sub> gas. These products are then separated and purified for partial reuse in manufacturing new PU materials. However, the costs associated with the separation and refinement of the hydrolytic products make this process unfavorable.<sup>148</sup>

**(ii) Acidolysis.** This process involves the depolymerization of PU into polyols in the presence of acids, such as dicarboxylic acids, at low temperatures (around 60 °C) for a short duration. The dicarboxylic acid acts as a cleavage agent, reacting with the carbamate bonds in the PU chain to break it down into polyols, oligomers with urea, and small molecules.<sup>149</sup> Gama *et al.*<sup>148</sup> successfully recycled PU using acidolysis with succinic acid as the depolymerizing agent. The resulting polyol was reused at a 30% ratio to produce new PU foam, which exhibited properties similar to foam made from 100% conventional polyol. In a separate study, Grdadolnik *et al.*<sup>150</sup> employed adipic acid for the acidolysis of FPU scrap without catalysts. Their results indicated that replacing commercial polyol with 50% recovered polyol enhanced the mechanical properties by 40% compared to foam made from 100% virgin polyol.

**(iii) Aminolysis.** This method involves the decomposition of urethane bonds to polyol and disubstituted urea in the presence of amines such as ethanol amine or dibutyl amine. The end products are amines and oligomeric urea. However, side reactions and the challenge of separating amines from the products are significant drawbacks of this method. Grdadolnik *et al.*<sup>151</sup> used tris(2-aminoethyl)amine for the aminolysis of FPU waste and successfully reused it in the production of FPU foam. Their results indicated that FPU made from 100% recovered polyol demonstrated greater mechanical performance compared to FPU made from 100% virgin polyol.

**(iv) Glycolysis.** This method employs high-boiling glycols as the depolymerization reagent.<sup>152</sup> The urethane linkages are broken down by the active hydrogen atoms in the glycol structure. It is currently the most favored recycling method due to its straightforward process. However, its disadvantages include high energy requirements and lengthy processing times, which limit its industrial application.<sup>149</sup> Polyols recovered from split-phase glycolysis exhibit enhanced properties and higher purity compared to those obtained from single-phase glycolysis. The solubility of the polyols in the glycol is critical for the separation of the two phases. In this method, the upper phase predominantly consists of the recovered polyols, whereas the bottom phase contains the excess glycol and other reaction byproducts.<sup>152</sup> Several studies have been conducted to improve the efficiency of the glycolysis method for recycling PUs. Molero *et al.*<sup>153</sup> investigated the use of diethylene glycol (DEG) with potassium octoate as a catalyst to speed up the recycling process. The recovered polyol was reused in PU production and compared to PU made from 100% conventional polyol. The results indicated that incorporating 25% recovered polyol into the PU formulation did not negatively affect the foam morphology. In other study, Vanbergen *et al.*<sup>140</sup> achieved high purity polyol by using glycerol for depolymerization of FPU scrap, with lactam as a process accelerator. The recovered polyol was reused in new FPU foam production, and their

findings showed that incorporating up to 50% recovered polyol did not affect the foam's cellular structure.

When comparing the two primary methods of PU recycling, mechanical recycling stands out as a simpler, scalable, and cost-effective option that requires minimal energy compared to chemical recycling. The material obtained through mechanical recycling is characterized by a higher density and reduced flexibility and deformability when compared to FPU foam. This material is extensively employed in the fields of furniture, packaging, automotive manufacturing, sound attenuation, and impact resistance applications. However, mechanical recycling does not involve breaking down PU into its original chemical constituents. Instead, it repurposes shredded foam scraps to create new materials with varying densities, tailored to diverse industrial applications based on processing parameters. This technique is also environmentally sustainable, as it produces no detrimental emissions. In contrast, chemical recycling takes a fundamentally different approach, breaking down PU chains into their original chemical constituents, such as polyols, amines, and isocyanates. This method offers higher recycling efficiency by regenerating raw materials that can be reused to manufacture new PU products. However, chemical recycling is energy-intensive, requires precise control of reaction conditions, and relies on various chemicals, making it complex, costly, and less scalable. The quality and performance of FPU foam derived from recovered polyols are significantly influenced by the efficacy of the recovery process and the purity of the recovered polyols. Studies demonstrate that the characteristics of FPU foam made from recovered polyols are often comparable to,<sup>144</sup> or even better than,<sup>151</sup> those of virgin foam.

## 8. Application of FPU foam in energy harvesting

As the global economy continues to expand rapidly, coupled with the limited availability of fossil fuels and the escalating issue of environmental pollution, there is an ever-growing demand for energy sources that are efficient but also clean and sustainable. Nanogenerators (NGs) are an exciting new category of energy-harvesting devices that promise to harness energy from the surrounding environment, such as light, heat, or mechanical vibrations. Of these, the use of a triboelectric nanogenerator (TENG), developed by Wang in 2012,<sup>47</sup> is a new approach in this field based on triboelectrification and electrostatic induction between two dissimilar materials. TENGs are distinguished by their high efficiency, significant output power, affordability, and simplicity of production. There are four operating modes of TENGs:<sup>154</sup> vertical contact-separation mode (Fig. 10a), in-plane contact-sliding mode (Fig. 10b), freestanding triboelectric-layer mode (Fig. 10c), and single-electrode mode (Fig. 10d). Among them, vertical contact-separation is the most employed approach due to its ability to generate a high output voltage. The triboelectric effect is utilized to produce electrical energy by means of periodic vertical contact and separation between two distinct materials. Fig. 11





Fig. 10 Four operating modes of TENGs.

illustrates the working principle of a TENG employing a contact-separation mode. In the initial state, neither charge generation nor induction occurs, as demonstrated in Fig. 11a. When the surfaces of two distinct materials come into contact, triboelectric charges are produced, as shown in Fig. 11b. Subsequently, as the two contacted surfaces separate, a potential difference is established, leading to an instant flow of electrons from the bottom electrode to the top electrode, as depicted in Fig. 11c. Equilibrium is attained when the two surfaces are completely separated, as revealed in Fig. 11d. Upon pressing the two surfaces together once more, the electrostatic-induced charges will return through the external load to equalize the electric potential difference, as illustrated in Fig. 11e. The TENG can be

operated repeatedly by periodically bringing the materials into contact and separating them, enabling continuous electrical energy generation.<sup>30,155–157</sup> However, the output voltage of the TENG device is based on the applied force, contact frequency, contact area, and type of materials used.<sup>158,159</sup>

The primary materials commonly used in TENG devices can be categorized into tribopositive and tribonegative materials. Tribopositive materials tend to donate electrons, while tribonegative materials tend to accept electrons.<sup>160</sup> Metals like aluminum (Al), copper (Cu), and silver (Ag) are frequently employed as tribopositive materials, while polymeric-based materials such as polytetrafluoroethylene (PTFE), polyethylene-terephthalate (PET), polydimethylsiloxane (PDMS), polyimide



Fig. 11 Working principle of vertical contact-separation mode.



(PI), and polyvinylidene fluoride (PVDF) are commonly used as tribonegative materials. However, metals are prone to oxidation and corrosion in harsh environments, which can adversely impact the performance and durability of TENG devices. To address this issue, various polymeric materials like polyurethanes (PUs),<sup>16</sup> polypyrrole,<sup>161</sup> cellulose,<sup>162</sup> and polyamide<sup>163</sup> have been utilized as tribopositive materials due to their adaptability, low cost, high ability to donate electrons and resistance to environmental degradation.<sup>164</sup> For instance, Wang *et al.*<sup>164</sup> successfully utilized polypyrrole as a tribopositive material paired with PTFE as the tribonegative material in a TENG device, achieving notable performance such as an output voltage of 52 V at 10 Hz, an output current density of 45 mA m<sup>-2</sup> at 10 Hz, and a maximum power density of 5.8 W m<sup>-2</sup> at a resistance of 400 MΩ. Although polymeric materials generally exhibit lower performance compared to metals in TENG devices, researchers have explored innovative approaches to enhance their efficiency. Zheng *et al.*<sup>165</sup> demonstrated the use of porous materials, chitosan aerogel film and polyimide, in a TENG, resulting in an output voltage of 60.6 V, a current of 7.7 μA, and a power density of 2.33 W m<sup>-2</sup>. In another study, Wang *et al.*<sup>166</sup> investigated the impact of porous PTFE on the electrical output of the TENG and compared it with the outputs obtained using solid PTFE (with no porosity) in the TENG. The results showed that the output voltage of the TENG utilizing porous PTFE was 1.8 times higher than that of the TENG using solid PTFE under identical oscillation conditions. Saadatnia *et al.*<sup>167</sup> created a porous polyimide-based TENG, where the porosity of the polyimide varied from 0 to 50%. The results indicated that the output voltage, output current, and power were 40 V, 5 μA, and 47 μW, respectively, at 50% porosity. This was significantly higher than the solid polyimide film, with an enhancement of 8 times. These studies emphasized the greater efficiency of porous materials in TENG devices, as they facilitate charge generation not only on the surface as in dense materials but also within the inner pores, thereby enhancing electrostatic induction and overall device performance.

Different types of porous materials such as polystyrene foam,<sup>168</sup> PDMS sponge,<sup>169</sup> PVDF,<sup>170</sup> PTFE<sup>166</sup> and FPU foam<sup>171</sup> have been investigated as triboelectric layers in TENG devices. Table 5 summarizes the output performance of TENG devices using different porous materials.

In recent years, there has been a growing interest in incorporating FPU foam into TENG devices. FPU foam offers several advantages that make it well-suited for TENG applications including flexibility, lightweight, elasticity, deformability, versatility, tailored density, durability, and robustness.<sup>51,171,176,177</sup> This adaptability enables the integration of TENG devices into wearable electronics, intelligent textiles, and other flexible devices, thereby expanding energy harvesting applications.<sup>48</sup> Several studies have been conducted to improve the electrical properties of FPU foam. For instance, Weldemhret *et al.*<sup>48</sup> demonstrated how carbon loading can influence the electrical performance of FPU foam when used in a TENG device. Their results showed that with a carbon loading of 40 wt%, FPU/carbon composites could be integrated into a shoe's insole, generating 36 V and 100 V when walking and running, respectively, at a contact force of 20 N, and a frequency of 6 Hz. Liu *et al.*<sup>171</sup> developed a conductive elastic sponge (ES) coated with polyaniline nanowires (PANI NWS) to effectively harvest irregular and random mechanical energy using a TENG device. The study investigated the impact of deformation levels (2% to 60%) and PANI coating time (6 to 48 hours) on the ES-TENG's performance. The results showed that at a 60% deformation level, the ES-TENG achieved a maximum output of 540 V and 6 μA. As the PANI polymerization time increased, the output voltage, current, and charge density also increased, demonstrating the benefits of the porous sponge structure and PANI nanowires in enhancing triboelectric efficiency through a larger contact area. Furthermore, the conductive PANI coating allowed the ES-TENG to function as a self-powered ammonia (NH<sub>3</sub>) sensor, exhibiting high sensitivity and rapid response time. Weldemhret *et al.*<sup>30</sup> studied the effect of a phosphorus-doped mesoporous carbon (PMC)-filled coating on FPU foam and its impact on the output performance of a TENG. The results demonstrated good energy harvesting performance, with an open-circuit voltage of 158 V and a short-circuit current density of 2.26 μA cm<sup>-2</sup>. Saadatnia *et al.*<sup>51</sup> fabricated a high-performance TENG based on porous PU aerogel. The findings demonstrated significantly improved electrical output characteristics, 3.5 times higher compared to non-porous films, making it suitable for energy harvesting applications and as a biomechanical sensor for monitoring arm motion. The current

Table 5 Comparison of the output performance of TENG devices using different porous materials

Material	Output voltage (V)	Output current (μA)	Contact area (cm <sup>2</sup> )	Power density (mW cm <sup>-2</sup> )	Applied force/contact frequency (N/Hz)	Ref.
PDMS sponge	181	2.26	3.7 × 3.7	0.089	6/1.6	169
Polystyrene foam	130	100	1 × 1	—	90/10	168
Recycled polystyrene/ZnO	8.2	10	2 × 1	0.0281	4/10	172
Porous PVDF	90	15	1 × 2	0.615	16/10	170
Porous polyimide film	40	5	2 × 2	0.01175	—/5	167
TPU nanofiber	5.8	7.28	5 × 5	0.0009	5/8	173
PANI NWS@FPU	540	6	8 × 5	0.007	—/6	171
FPU/carbon nanocomposite	130.6	15.6	2 × 2	—	20/6	48
FPU/MMT nanocomposite	164	11.5	9 × 5	0.0328	4.8/5	16
FPU (density 33 kg m <sup>-3</sup> )	273	10.2	8 × 5.5	0.025	4.8/5	174
Rebonded FPU (density 60 kg m <sup>-3</sup> )	117	28	7 × 5.5	0.085	4.7/5	175



authors modified FPU foam by adding varying amounts (0.1, 0.3, 0.5, and 0.7% by weight) of natural montmorillonite (Na-MMT) nanoclay. When the FPU/Na-MMT0.3 composite was subjected to a force of 4.8 N at a frequency of 5 Hz, it generated an output voltage of 164 V, representing a 62.37% increase compared to the unmodified FPU foam.<sup>16</sup> In a separate study, the current authors explored how varying densities (17, 22, 26, and 33 kg m<sup>-3</sup>) and thicknesses (4, 6, 8, and 10 mm) of FPU foam affect the performance of a TENG device. The density of the FPU foam was adjusted by changing the isocyanate index (1.05, 1.10, 1.15, and 1.20) and water content. The findings revealed that the highest output voltage of 273 V was achieved with the highest density (33 kg m<sup>-3</sup>) and the lowest thickness (4 mm) at a contact frequency of 5 Hz and an applied force of 4.8 N. Under the same conditions, the maximum power density recorded was 0.025 mW cm<sup>-2</sup> at a resistance of 20 MΩ. Additionally, the FPU-based TENG device successfully powered four white LEDs connected in series.<sup>174</sup>

The concept of waste-to-energy, as proposed by the US Environmental Protection Agency (USEPA) and the Energy Information Administration (EIA), promotes not only a cleaner environment but also clean and sustainable energy. In addition to virgin materials, numerous studies have highlighted the effectiveness of recycled waste materials as triboelectric layers, exhibiting high output performance in TENG applications.<sup>178-180</sup> However, the chemical processing required for the fabrication of these materials often introduces additional complexity, increases costs, and extends the processing time. Therefore, the selection of waste materials and recycling technique employed are critical factors to consider prior to their utilization in TENG devices. The current authors used two distinct densities of rebonded FPU scraps, 60 and 70 kg m<sup>-3</sup>, as tribopositive sheets in a TENG device. The rebonded FPU was developed using mechanical compression with MDI as a binder. The results revealed that rebonded FPU with a density of 60 kg m<sup>-3</sup> had a higher output voltage of 117 V than rebonded FPU with a density of 70 kg m<sup>-3</sup>. Furthermore, the power density was found to reach a maximum value of 0.085 mW cm<sup>-2</sup> at a load resistance of 5 MΩ and frequency of 5 Hz contact frequency. The rebonded FPU-based TENG device charged a 10 μF capacitor to 16 V in 25 seconds, indicating fast charging.<sup>175</sup> These findings showed an improvement over previously reported results using different waste materials.<sup>155,181,182</sup> Furthermore, the technique of synthesizing rebonded FPU was simpler and less expensive than that of other waste materials discussed in the literature, which involve chemical treatments that complicate and increase the cost of production. Thus, the rebonded FPU demonstrated promising potential as a material for use in TENG devices, enabling efficient and sustainable energy harvesting for powering wearable and flexible devices.

## 9. Conclusions and future prospects

The versatility and adaptability of FPU foams have established them as a crucial material in diverse applications. A review of

published studies on the utilization of FPU foam in energy harvesting highlights its significant potential in this field, primarily due to its unique characteristics, including its lightweight nature, deformability, adaptability, and elasticity, which collectively enhance its performance in energy harvesting applications. However, the review of the current literature revealed that the use of FPU foams in TENG devices is limited by several constraints that require future attention. The operational output of FPU based-TENG devices is susceptible to fluctuations due to environmental conditions such as temperature, humidity, and other external factors. Accordingly, it is essential to conduct research to assess the effect of environmental conditions on the FPU foam TENG performance as these factors are expected to directly influence the operational efficiency of TENGs. Additionally, the high volume-to-mass ratio of FPU foam results in larger device sizes, which can be a significant drawback and can limit its applications. This was highlighted by the current authors who reported that a thinner FPU material (4 mm) performed better in terms of generating higher output voltage from the TENG device compared to a thicker FPU material (10 mm). Therefore, it is crucial to carefully select and adjust the thickness of the FPU material to optimize the performance of the TENG device for specific application needs, ensuring maximum efficiency and effectiveness in energy harvesting. Moreover, the electrical outputs of the TENG device depend on the pore morphology of the FPU foam, making it crucial to control it during preparation. Therefore, the control of pore architecture during the synthesis process becomes a critical factor to consider when adjusting the formulations by balancing between gelling and blowing reactions. This requires expertise in the synthesis of FPU foam with well controlled density and pore structure. Additionally, the mechanical durability and longevity of the FPU foam can deteriorate over time due to bacterial attack, leading to mechanical loss over extended periods. Aerobic microorganisms can proliferate within FPU foams in environments characterized by high humidity and oxygen content, thereby compromising their elasticity and deformability. Given the increasing use of FPU foam, its applicability could be extended to situations where antibacterial properties are crucial for effective long-term durability. Therefore, researchers should consider this issue and thoroughly comprehend its influence.

The use of various organic and inorganic fillers was reported to enhance the durability, thermal resistance, mechanical performance and electrical outputs of FPU foam. Fillers can also act as additional charges on the foam surface, increasing its electrical output. Despite the existing research incorporating various micron-sized and nanofillers, additional studies involving other nanofillers are desired.

Finally, it is important not to overlook that the production of PU foam relies heavily on petroleum feedstock, polyol, and isocyanate, necessitating a shift to renewable-based materials to protect the environment. Researchers are investigating alternative bio-based or recycled sources for polyol and diisocyanates to minimize the material's environmental impact. Furthermore, recycling of PU foams is crucial to mitigate the



environmental consequences of PU waste disposal through landfill or incineration. The use of recycled FPU foam instead of virgin PU foam in energy harvesting applications should be encouraged as it offers additional energy savings linked to the substantial impact of virgin materials on the total embodied energy in PU foam.

## Data availability

No primary research results, software or code have been included and no new data were generated or analysed as part of this review.

## Conflicts of interest

There are no conflicts to declare.

## Acknowledgements

This research was supported by the American University in Cairo under the internal grant agreement number SSE-MENG-A.E-FY22-RG-2022-Nov-10-19-38-38.

## References

- O. Bayer, *Angew. Chem.*, 1947, **59**, 257–272.
- A. Kemonia and M. Piot, *Polymers*, 2020, **12**, 1752.
- A. Maamoun and A. Mahmoud, *Cellulose*, 2022, **29**, 6323–6338.
- S. Dutta and N. Karak, *Prog. Org. Coat.*, 2005, **53**, 147–152.
- S. Thakur and N. Karak, *Prog. Org. Coat.*, 2013, **76**, 157–164.
- S. D. Desai, J. V. Patel and V. K. Sinha, *Int. J. Adhes. Adhes.*, 2003, **23**, 393–399.
- S. Sahoo, S. Mohanty and S. K. Nayak, *J. Macromol. Sci., Part A: Pure Appl. Chem.*, 2018, **55**, 36–48.
- H. Ding, C. Xia, J. Wang, C. Wang and F. Chu, *J. Mater. Sci.*, 2016, **51**, 5008–5018.
- D. Shen, S. Shi, T. Xu, X. Huang, G. Liao and J. Chen, *Constr. Build. Mater.*, 2018, **174**, 474–483.
- V. Kanyanta and A. Ivankovic, *J. Mech. Behav. Biomed. Mater.*, 2010, **3**, 51–62.
- Z. S. Petrović and J. Ferguson, *Prog. Polym. Sci.*, 1991, **16**, 695–836.
- H. Somarathna, S. Raman, D. Mohotti, A. Mutalib and K. Badri, *Constr. Build. Mater.*, 2018, **190**, 995–1014.
- M. Zhao, L. Hu, L. Dai, Z. Wang, J. He, Z. Wang, J. Chen, D. Hrynsphan and S. Tatsiana, *Bioresour. Technol.*, 2022, **345**, 126427.
- M. Indumathi and G. Rajarajeswari, *Int. J. Biol. Macromol.*, 2019, **124**, 163–174.
- J. Moon, S. B. Kwak, J. Y. Lee and J. S. Oh, *Elastomers Compos.*, 2017, **52**, 249–256.
- A. A. Maamoun, D. M. Naeim, A. A. Mahmoud, A. M. Esawi and M. Arafa, *Nano Energy*, 2024, **124**, 109426.
- H. W. Engels, H. G. Pirkl, R. Albers, R. W. Albach, J. Krause, A. Hoffmann, H. Casselmann and J. Dormish, *Angew. Chem., Int. Ed.*, 2013, **52**, 9422–9441.
- Precedence Research, Polyurethane Market Size and Companies, <https://www.precedenceresearch.com/polyurethane-market>, accessed 2nd April 2024.
- M. Charlon, B. Heinrich, Y. Matter, E. Couzigné, B. Donnio and L. Avérous, *Eur. Polym. J.*, 2014, **61**, 197–205.
- M. Szycher, *Szycher's handbook of polyurethanes*, CRC Press, 1999.
- A. Das and P. Mahanwar, *Adv. Ind. Eng. Polym. Res.*, 2020, **3**, 93–101.
- A. B. Morgan, *Fire Mater.*, 2021, **45**, 68–80.
- P. Scarfato, L. Di Maio and L. Incarnato, *Composites, Part B*, 2017, **109**, 45–52.
- R. Deng, P. Davies and A. Bajaj, *J. Sound Vib.*, 2003, **262**, 391–417.
- S. D. Bote, A. Kiziltas, I. Scheper, D. Mielewski and R. Narayan, *J. Appl. Polym. Sci.*, 2021, **138**, 50690.
- J. Moon, S. B. Kwak, J. Y. Lee, D. Kim, J. U. Ha and J. S. Oh, *Waste Manage.*, 2019, **85**, 557–562.
- J. G. Gwon, S. K. Kim and J. H. Kim, *Mater. Des.*, 2016, **89**, 448–454.
- G. Sung, S. K. Kim, J. W. Kim and J. H. Kim, *Polym. Test.*, 2016, **53**, 156–164.
- R. Verdejo, R. Stämpfli, M. Alvarez-Lainez, S. Mourad, M. Rodriguez-Perez, P. Brühwiler and M. Shaffer, *Compos. Sci. Technol.*, 2009, **69**, 1564–1569.
- T. G. Weldemhret, D.-W. Lee, M. Prabhakar, Y. T. Park and J. I. Song, *ACS Appl. Nano Mater.*, 2022, **5**, 12464–12476.
- M. Ionescu, *Chemistry and technology of polyols for polyurethanes*, iSmithers Rapra Publishing, 2005.
- C. Fang, X. Zhou, Q. Yu, S. Liu, D. Guo, R. Yu and J. Hu, *Prog. Org. Coat.*, 2014, **77**, 61–71.
- Y. Savelyev, V. Veselov, L. Markovskaya, O. Savelyeva, E. Akhranovich, N. Galatenko, L. Robota and T. Travinskaya, *Mater. Sci. Eng., C*, 2014, **45**, 127–135.
- D. K. Chattopadhyay and K. Raju, *Prog. Polym. Sci.*, 2007, **32**, 352–418.
- N. Taheri and S. Sayyahi, *e-Polymers*, 2016, **16**, 65–73.
- R. Patel, M. Shah and H. Patel, *Int. J. Polym. Anal. Charact.*, 2011, **16**, 107–117.
- D. Randall and S. Lee, *The polyurethanes book*, John Wiley & Sons, New York, NY, USA, 2002.
- D. Choi, Y. Lee, Z.-H. Lin, S. Cho, M. Kim, C. K. Ao, S. Soh, C. Sohn, C. K. Jeong and J. Lee, *ACS Nano*, 2023, **17**, 11087–11219.
- M. Hamlehdar, A. Kasaeian and M. R. Safaei, *Renewable Energy*, 2019, **143**, 1826–1838.
- X. Zhang, H. S. Chen and P. Yang, *Nano Energy*, 2024, **120**, 109160.
- J.-A. Choi, J. Jeong, M. Kang, H.-J. Ko, T. Kim, K. Park, J. Kim and S. Pyo, *Nano Energy*, 2024, **119**, 109071.
- Y. Cao, Y. Meng, Y. Jiang, S. Qian, D. Fan, X. Zhou, Y. Qian, S. Lin, T. Qian and Q. Pan, *Chem. Eng. J.*, 2022, **433**, 134549.
- Y. Meng, Y. Liu, Z. Wan, Y. Huan, Q. Guo, D. Fan, X. Zhou, J. Liu, Y. Cao and X. Cao, *Chem. Eng. J.*, 2023, **453**, 139967.



- 44 H. Zhu, M. Gu, X. Dai, S. Feng, T. Yang, Y. Fan, J. Zhang, D. Fan, Y. Liu and Y. Lu, *Chem. Eng. J.*, 2024, **494**, 153235.
- 45 Z. Yu, Z. Zhu, Y. Zhang, X. Li, X. Liu, Y. Qin, Z. Zheng, L. Zhang and H. He, *Carbohydr. Polym.*, 2024, **334**, 122040.
- 46 X. Tang, X. Wang, R. Cattley, F. Gu and A. D. Ball, *Sensors*, 2018, **18**, 4113.
- 47 F.-R. Fan, Z.-Q. Tian and Z. L. Wang, *Nano Energy*, 2012, **1**, 328–334.
- 48 T. G. Weldemhret, D.-W. Lee, Y. T. Park and J. I. Song, *Chem. Eng. J.*, 2022, **450**, 137982.
- 49 Z. L. Wang, *ACS Nano*, 2013, **7**, 9533–9557.
- 50 H. Zhang, Y. Lu, A. Ghaffarinejad and P. Basset, *Nano Energy*, 2018, **51**, 10–18.
- 51 Z. Saadatnia, S. G. Mosanenzadeh, T. Li, E. Esmailzadeh and H. E. Naguib, *Nano Energy*, 2019, **65**, 104019.
- 52 J. Zheng, X. Wei, Y. Li, W. Dong, X. Li, E. Shiju, Z. Wu and J. Wen, *Nano Energy*, 2021, **89**, 106397.
- 53 C. Defonseka, *Water-Blown Cellular Polymers: A Practical Guide*, Walter de Gruyter GmbH & Co KG, 2019.
- 54 E. Sharmin and F. Zafar, *Polyurethane*, 2012, **3**, 16.
- 55 T. Nakajima-Kambe, Y. Shigeno-Akutsu, N. Nomura, F. Onuma and T. Nakahara, *Appl. Microbiol. Biotechnol.*, 1999, **51**, 134–140.
- 56 J. O. Akindoyo, M. Beg, S. Ghazali, M. Islam, N. Jeyaratnam and A. Yuvaraj, *RSC Adv.*, 2016, **6**, 114453–114482.
- 57 M. Zieleniewska, M. K. Leszczyński, L. Szczepkowski, A. Bryskiewicz, M. Krzyżowska, K. Bień and J. Ryszkowska, *Polym. Degrad. Stab.*, 2016, **132**, 78–86.
- 58 T. Miyajima, K. Nishiyama, M. Satake and T. Tsuji, *Polym. J.*, 2015, **47**, 771–778.
- 59 J. Herzberger, K. Niederer, H. Pohlit, J. Seiwert, M. Worm, F. R. Wurm and H. Frey, *Chem. Rev.*, 2016, **116**, 2170–2243.
- 60 J. Blankenburg, E. Kersten, K. Maciol, M. Wagner, S. Zorbakhsh and H. Frey, *Polym. Chem.*, 2019, **10**, 2863–2871.
- 61 M. Ates, S. Karadag, A. A. Eker and B. Eker, *Polym. Int.*, 2022, **71**, 1157–1163.
- 62 Z. Khan, F. Javed, Z. Shamair, A. Hafeez, T. Fazal, A. Aslam, W. B. Zimmerman and F. Rehman, *J. Ind. Eng. Chem.*, 2021, **103**, 80–101.
- 63 X. Zhang, D. A. MacDonald, M. F. Goosen and K. B. McAuley, *J. Polym. Sci., Part A: Polym. Chem.*, 1994, **32**, 2965–2970.
- 64 M. De Jong, R. Feijt, E. Zondervan, T. Nijhuis and A. De Haan, *Appl. Catal.*, 2009, **365**, 141–147.
- 65 C. Song, Y. Qi, T. Deng, X. Hou and Z. Qin, *Renewable Energy*, 2010, **35**, 625–628.
- 66 F. E. Golling, R. Pires, A. Hecking, J. Weikard, F. Richter, K. Danielmeier and D. Dijkstra, *Polym. Int.*, 2019, **68**, 848–855.
- 67 S. Rabbani, E. Bakhshandeh, R. Jafari and G. Momen, *Prog. Org. Coat.*, 2022, **165**, 106715.
- 68 M. Malaki, Y. Hashemzadeh and M. Karevan, *Prog. Org. Coat.*, 2016, **101**, 477–485.
- 69 J. Zhang and C. P. Hu, *Eur. Polym. J.*, 2008, **44**, 3708–3714.
- 70 F. M. de Souza, P. K. Kahol and R. K. Gupta, *Polyurethane Chemistry: Renewable Polyols and Isocyanates*, ACS Publications, 2021, pp. 1–24.
- 71 Z. S. Petrović, *Polym. Rev.*, 2008, **48**, 109–155.
- 72 Grand View Research, Bio-Based Polyurethane Industry Analysis, <https://www.grandviewresearch.com/industry-analysis/bio-based-polyurethane-industry>, accessed 20 May, 2024.
- 73 M. A. Aristri, M. A. R. Lubis, S. M. Yadav, P. Antov, A. N. Papadopoulos, A. Pizzi, W. Fatriasari, M. Ismayati and A. H. Iswanto, *Appl. Sci.*, 2021, **11**, 4242.
- 74 A. Tenorio-Alfonso, M. C. Sánchez and J. M. Franco, *J. Polym. Environ.*, 2020, **28**, 749–774.
- 75 B. Freedman, E. Pryde and T. Mounts, *J. Am. Oil Chem. Soc.*, 1984, **61**, 1638–1643.
- 76 V. V. Goud, A. V. Patwardhan and N. C. Pradhan, *Bioresour. Technol.*, 2006, **97**, 1365–1371.
- 77 A. Noreen, K. M. Zia, M. Zuber, S. Tabasum and A. F. Zahoor, *Prog. Org. Coat.*, 2016, **91**, 25–32.
- 78 M. Spontón, N. Casis, P. Mazo, B. Raúd, A. Simonetta, L. Rios and D. Estenoz, *Int. Biodeterior. Biodegrad.*, 2013, **85**, 85–94.
- 79 D. Gurgel, D. Bresolin, C. Sayer, L. Cardozo Filho and P. H. H. de Araújo, *Ind. Crops Prod.*, 2021, **164**, 113377.
- 80 J. John, M. Bhattacharya and R. B. Turner, *J. Appl. Polym. Sci.*, 2002, **86**, 3097–3107.
- 81 L. Zhang, H. K. Jeon, J. Malsam, R. Herrington and C. W. Macosko, *Polymer*, 2007, **48**, 6656–6667.
- 82 A. Prociak, E. Malewska, M. Kurańska, S. Bąk and P. Budny, *Ind. Crops Prod.*, 2018, **115**, 69–77.
- 83 H. Pawlik and A. Prociak, *J. Polym. Environ.*, 2012, **20**, 438–445.
- 84 P. Rojek and A. Prociak, *J. Appl. Polym. Sci.*, 2012, **125**, 2936–2945.
- 85 M. Zieleniewska, M. K. Leszczyński, M. Kurańska, A. Prociak, L. Szczepkowski, M. Krzyżowska and J. Ryszkowska, *Ind. Crops Prod.*, 2015, **74**, 887–897.
- 86 V. R. Da Silva, M. A. Mosiewicki, M. I. Yoshida, M. C. Da Silva, P. M. Stefani and N. E. Marcovich, *Polym. Test.*, 2013, **32**, 438–445.
- 87 W. Zhou, C. Bo, P. Jia, Y. Zhou and M. Zhang, *Polymers*, 2018, **11**, 45.
- 88 S. Dworakowska, A. Cornille, D. Bogdal, B. Boutevin and S. Caillol, *Materials*, 2022, **15**, 628.
- 89 S. Miao, S. Zhang, Z. Su and P. Wang, *J. Appl. Polym. Sci.*, 2013, **127**, 1929–1936.
- 90 P. T. Wai, P. Jiang, Y. Shen, P. Zhang, Q. Gu and Y. Leng, *RSC Adv.*, 2019, **9**, 38119–38136.
- 91 I. Singh, S. K. Samal, S. Mohanty and S. K. Nayak, *Eur. J. Lipid Sci. Technol.*, 2020, **122**, 1900225.
- 92 M. F. Sonnenschein, *Polyurethanes: science, technology, markets, and trends*, John Wiley & Sons, 2021.
- 93 R. H. Richter and R. D. Priester Jr, *Kirk-Othmer Encyclopedia of Chemical Technology*, 2000.
- 94 S.-T. Lee and N. S. Ramesh, *Polymeric foams: mechanisms and materials*, CRC Press, 2004.
- 95 C. Defonseka, *Practical guide to flexible polyurethane foams*, Smithers Rapra, 2013.
- 96 R. Van Maris, Y. Tamano, H. Yoshimura and K. M. Gay, *J. Cell. Plast.*, 2005, **41**, 305–322.
- 97 S. Dworakowska, D. Bogdał, F. Zaccheria and N. Ravasio, *Catal. Today*, 2014, **223**, 148–156.



- 98 A. Strachota, B. Strachotová and M. Špírková, *Mater. Manuf. Processes*, 2008, **23**, 566–570.
- 99 Y. Zhao, F. Zhong, A. Tekeci and G. J. Suppes, *Appl. Catal., A*, 2014, **469**, 229–238.
- 100 A. Guo, I. Javni and Z. Petrovic, *J. Appl. Polym. Sci.*, 2000, **77**, 467–473.
- 101 T. Kattiyaboot and C. Thongpin, *Energy Procedia*, 2016, **89**, 177–185.
- 102 B. Grüning and G. Koerner, *Tenside, Surfactants, Deterg.*, 1989, **26**, 312–317.
- 103 X. Zhang, C. Macosko, H. Davis, A. Nikolov and D. Wasan, *J. Colloid Interface Sci.*, 1999, **215**, 270–279.
- 104 K. Ashida, *Polyurethane and related foams: chemistry and technology*, CRC Press, 2006.
- 105 N. Malwitz, S.-W. Wong, K. Frisch and P. Manis, *J. Cell. Plast.*, 1987, **23**, 461–502.
- 106 A. L. Silva and J. C. Bordado, *Catal. Rev.*, 2004, **46**, 31–51.
- 107 H. Choe, G. Sung and J. H. Kim, *Compos. Sci. Technol.*, 2018, **156**, 19–27.
- 108 Q. Wu, J. Zhang, S. Wang, B. Chen, Y. Feng, Y. Pei, Y. Yan, L. Tang, H. Qiu and L. Wu, *Front. Chem. Sci. Eng.*, 2021, **15**, 969–983.
- 109 D. Fan, N. Li, M. Li, S. Wang, S. Li and T. Tang, *Chem. Eng. J.*, 2022, **427**, 131635.
- 110 T. G. Weldemhret, D. W. Lee, P. MN, A. Iqbal, C. M. Koo, Y. T. Park and J. I. Song, *Adv. Mater. Interfaces*, 2023, **10**, 2300461.
- 111 Y. Pan, L. Liu, W. Cai, Y. Hu, S. Jiang and H. Zhao, *Appl. Clay Sci.*, 2019, **168**, 230–236.
- 112 J. Lu, C. Liao, L. Cheng, P. Jia, Z. Yin, L. Song, B. Wang and Y. Hu, *J. Cleaner Prod.*, 2022, **333**, 130172.
- 113 B.-X. Zhang, Z.-L. Hou, W. Yan, Q.-L. Zhao and K.-T. Zhan, *Carbon*, 2017, **125**, 199–206.
- 114 Y. Shen, Z. Lin, J. Wei, Y. Xu, Y. Wan, T. Zhao, X. Zeng, Y. Hu and R. Sun, *Carbon*, 2022, **186**, 9–18.
- 115 M. Beccatelli, M. Villani, F. Gentile, L. Bruno, D. Seletti, D. M. Nikolaidou, M. Culiolo, A. Zappettini and N. Coppede, *ACS Appl. Polym. Mater.*, 2021, **3**, 1563–1572.
- 116 Y. Ding, J. Yang, C. R. Tolle and Z. Zhu, *ACS Appl. Mater. Interfaces*, 2018, **10**, 16077–16086.
- 117 J. Wicks, W. Zeno, F. N. Jones and S. Peppas, *Drying Technol.*, 1993, **11**, 1477.
- 118 A. Maamoun, A. El-Wakil and T. M. El-Basheer, *J. Cell. Plast.*, 2022, **58**, 645–672.
- 119 J. W. Cho and S. H. Lee, *Eur. Polym. J.*, 2004, **40**, 1343–1348.
- 120 H. Etemadi, S. Afsharkia, S. Zinatloo-Ajabshir and E. Shokri, *Polym. Eng. Sci.*, 2021, **61**, 2364–2375.
- 121 D. Chen, J. Yang and G. Chen, *Composites, Part A*, 2010, **41**, 1636–1638.
- 122 T.-Y. Yu, Y.-K. Tseng, T.-H. Lin, T.-C. Wang, Y.-H. Tseng, Y.-H. Chang, M.-C. Wu and W.-F. Su, *Carbohydr. Polym.*, 2022, **291**, 119549.
- 123 A. Hadjadj, O. Jbara, A. Tara, M. Gilliot, F. Malek, E. M. Maafi and L. Tighzert, *Compos. Struct.*, 2016, **135**, 217–223.
- 124 B. Krishnamurthi, S. Bharadwaj-Somaskandan, T. Sergeeva and F. Shutov, *Cell. Polym.*, 2003, **22**, 371–382.
- 125 I. Izarra, A. Borreguero, I. Garrido, J. Rodríguez and M. Carmona, *Polym. Test.*, 2021, **100**, 107268.
- 126 H. Liu, B. Zhang and J. Han, *RSC Adv.*, 2017, **7**, 35320–35329.
- 127 F. Feng and L. Qian, *Polym. Compos.*, 2014, **35**, 301–309.
- 128 Y. J. Kim, H. J. Kang, C. T. Moerk, B.-T. Lee, J. S. Choi and J.-H. Yim, *Sens. Actuators, B*, 2021, **344**, 130269.
- 129 C. Li, H. Ye, S. Ge, Y. Yao, B. Ashok, N. Hariram, H. Liu, H. Tian, Y. He and G. Guo, *J. Mater. Res. Technol.*, 2022, **19**, 3603–3615.
- 130 G. Kasi, S. Gnanasekar, K. Zhang, E. T. Kang and L. Q. Xu, *J. Appl. Polym. Sci.*, 2022, **139**, 52181.
- 131 S. Członka, A. Strąkowska and A. Kairytė, *Polym. Test.*, 2020, **87**, 106534.
- 132 S. Kiddell, Y. Kazemi, J. Sorken and H. Naguib, *Polym. Test.*, 2023, **119**, 107919.
- 133 A. Alis, R. A. Majid, I. A. A. Nasir, N. S. Mustaffa and W. H. W. Hassan, *AIP Conf. Proc.*, 2017, **1865**, 040005.
- 134 S. Członka, A. Strąkowska, A. Kairytė and A. Kremensas, *Polym. Test.*, 2020, **86**, 106479.
- 135 P. Bartczak, M. Wysokowski, K. Szylińczuk, M. Odalanowska, T. Jesionowski and S. Borysiak, *Ind. Crops Prod.*, 2023, **204**, 117237.
- 136 H. Olcay and E. D. Kocak, *Appl. Acoustics*, 2021, **173**, 107733.
- 137 V. R. da Silva, M. A. Mosiewicki, M. I. Yoshida, M. C. da Silva, P. M. Stefani and N. E. Marcovich, *Polym. Test.*, 2013, **32**, 665–672.
- 138 H. Olcay and E. D. Kocak, *J. Ind. Text.*, 2020, **51**, 8738S–8763S.
- 139 E. Akdogan and M. Erdem, *J. Polym. Res.*, 2021, **28**, 80.
- 140 J. Paciorek-Sadowska, M. Borowicz and M. Isbrandt, *Polymer*, 2023, **15**, 3529.
- 141 X. Zhou, M. M. Sain and K. Oksman, *Composites, Part A*, 2016, **83**, 56–62.
- 142 H. Chen, M. Zheng, H. Sun and Q. Jia, *Mater. Sci. Eng., A*, 2007, **445**, 725–730.
- 143 B. Adak, B. S. Butola and M. Joshi, *Appl. Clay Sci.*, 2018, **161**, 343–353.
- 144 T. Vanbergen, I. Verlent, J. De Geeter, B. Haelterman, L. Claes and D. De Vos, *ChemSusChem*, 2020, **13**, 3835–3843.
- 145 D. Simón, A. Borreguero, A. De Lucas and J. Rodríguez, *Waste Manage.*, 2018, **76**, 147–171.
- 146 K. M. Zia, H. N. Bhatti and I. A. Bhatti, *React. Funct. Polym.*, 2007, **67**, 675–692.
- 147 L. R. Mahoney, S. A. Weiner and F. C. Ferris, *Environ. Sci. Technol.*, 1974, **8**, 135–139.
- 148 N. Gama, B. Godinho, G. Marques, R. Silva, A. Barros-Timmons and A. Ferreira, *Chem. Eng. J.*, 2020, **395**, 125102.
- 149 N. V. Gama, A. Ferreira and A. Barros-Timmons, *Materials*, 2018, **11**, 1841.
- 150 M. Grdadolnik, A. Drincic, A. Oreski, O. C. Onder, P. Utrosa, D. Pahovnik and E. Zagar, *ACS Sustainable Chem. Eng.*, 2022, **10**, 1323–1332.
- 151 M. Grdadolnik, B. Zdovc, A. Drincic, O. C. Onder, P. Utrosa, S. G. Ramos, E. D. Ramos, D. Pahovnik and E. Zagar, *ACS Sustainable Chem. Eng.*, 2023, **11**, 10864–10873.
- 152 P. Zahedifar, L. Pazdur, C. M. Vande Velde and P. Billen, *Sustainability*, 2021, **13**, 3583.



- 153 C. Molero, A. De Lucas, F. Romero and J. Rodríguez, *J. Appl. Polym. Sci.*, 2008, **109**, 617–626.
- 154 T. Cheng, Q. Gao and Z. L. Wang, *Adv. Mater. Technol.*, 2019, **4**, 1800588.
- 155 G. M. Rani, C.-M. Wu, K. G. Motora and R. Umaphathi, *J. Cleaner Prod.*, 2022, **363**, 132532.
- 156 Y. Su, T. Yang, X. Zhao, Z. Cai, G. Chen, M. Yao, K. Chen, M. Bick, J. Wang and S. Li, *Nano Energy*, 2020, **74**, 104941.
- 157 V. Singh and B. Singh, *Polymer*, 2023, **274**, 125910.
- 158 Z. L. Wang, L. Lin, J. Chen, S. Niu, Y. Zi, Z. L. Wang, L. Lin, J. Chen, S. Niu and Y. Zi, *Triboelectr. nanogener.*, 2016, 23–47.
- 159 R. K. Cheedarala and K. K. Ahn, *Nano Energy*, 2018, **44**, 430–437.
- 160 P. Zhao, N. Soin, A. Kumar, L. Shi, S. Guan, C. Tsonos, Z. Yu, S. C. Ray, J. A. McLaughlin and Z. Zhu, *Nano Energy*, 2020, **67**, 104291.
- 161 J. Wang, Z. Wen, Y. Zi, P. Zhou, J. Lin, H. Guo, Y. Xu and Z. L. Wang, *Adv. Funct. Mater.*, 2016, **26**, 1070–1076.
- 162 C. Yao, X. Yin, Y. Yu, Z. Cai and X. Wang, *Adv. Funct. Mater.*, 2017, **27**, 1700794.
- 163 B. Cheng, C. Li, T. Ji, Y. Zhao, K. Gao, J. Hao and W. Xu, *Nano Energy*, 2024, **127**, 109718.
- 164 J. Wang, Z. Wen, Y. Zi, L. Lin, C. Wu, H. Guo, Y. Xi, Y. Xu and Z. L. Wang, *Adv. Funct. Mater.*, 2016, **26**, 3542–3548.
- 165 Q. Zheng, L. Fang, H. Guo, K. Yang, Z. Cai, M. A. B. Meador and S. Gong, *Adv. Funct. Mater.*, 2018, **28**, 1706365.
- 166 M. Wang, N. Zhang, Y. Tang, H. Zhang, C. Ning, L. Tian, W. Li, J. Zhang, Y. Mao and E. Liang, *J. Mater. Chem. A*, 2017, **5**, 12252–12257.
- 167 Z. Saadatnia, S. G. Mosanenzadeh, E. Esmailzadeh and H. E. Naguib, *Sci. Rep.*, 2019, **9**, 1370.
- 168 K. Y. Lee, J. Chun, J.-H. Lee, K. N. Kim, N.-R. Kang, J.-Y. Kim, M. H. Kim, K.-S. Shin, M. K. Gupta and J. M. Baik, *Adv. Mater.*, 2014, **26**, 5037–5042.
- 169 Z. Peng, J. Song, Y. Gao, J. Liu, C. Lee, G. Chen, Z. Wang, J. Chen and M. K. Leung, *Nano Energy*, 2021, **85**, 106021.
- 170 M. Wang, W. Liu, X. Shi, J. Pan, B. Zhou, J. Wang, T. Sun and Y. Tang, *New J. Chem.*, 2021, **45**, 1893–1898.
- 171 Y. Liu, Y. Zheng, Z. Wu, L. Zhang, W. Sun, T. Li, D. Wang and F. Zhou, *Nano Energy*, 2021, **79**, 105422.
- 172 D. Kamaruzaman, N. S. M. Mustakim, A. S. R. A. Subki, N. Parimon, M. K. Yaakob, M. F. Malek, N. Vasimalai, M. H. Abdullah, S. A. Bakar and M. K. Ahmad, *Mater. Today Sustainability*, 2024, **26**, 100726.
- 173 H. J. Oh, J. H. Bae, Y. K. Park, J. Song, D. K. Kim, W. Lee, M. Kim, K. J. Heo, Y. Kim and S. H. Kim, *Polymers*, 2020, **12**, 1044.
- 174 A. A. Maamoun, A. A. Mahmoud, D. Naeim, M. Arafa and A. Esawi, *Mater. Adv.*, 2024, **5**, 6132–6144.
- 175 A. A. Maamoun, A. M. Esawi, A. A. Mahmoud, D. M. Naeim and M. Arafa, *Appl. Energy*, 2025, **377**, 124579.
- 176 Z. Wu, P. Wang, B. Zhang, H. Guo, C. Chen, Z. Lin, X. Cao and Z. L. Wang, *Adv. Mater. Technol.*, 2021, **6**, 2000737.
- 177 H. Li, T. K. Sinha, J. S. Oh and J. K. Kim, *ACS Appl. Mater. Interfaces*, 2018, **10**, 14008–14016.
- 178 M. Sahu, S. Hajra, H.-G. Kim, H.-G. Rubahn, Y. K. Mishra and H. J. Kim, *Nano Energy*, 2021, **88**, 106255.
- 179 M. Navaneeth, S. Potu, A. Babu, B. Lakshakoti, R. K. Rajaboina, U. Kumar K, H. Divi, P. Kodali and K. Balaji, *ACS Sustainable Chem. Eng.*, 2023, **11**, 12145–12154.
- 180 B. Dudem, R. I. G. Dharmasena, R. Riaz, V. Vivekananthan, K. Wijyantha, P. Lugli, L. Petti and S. R. P. Silva, *ACS Appl. Mater. Interfaces*, 2022, **14**, 5328–5337.
- 181 N. R. Alluri, N. P. M. J. Raj, G. Khandelwal, V. Vivekananthan and S.-J. Kim, *Nano Energy*, 2020, **73**, 104767.
- 182 G. Khandelwal, A. Chandrasekhar, N. R. Alluri, V. Vivekananthan, N. P. M. J. Raj and S.-J. Kim, *Appl. Energy*, 2018, **219**, 338–349.

